1. Introduction

The brain–computer interface (BCI) or brain–machine interface (BMI) is an interface technology that enables communication with others and control of the environment or of a prosthesis without any muscle movement (Wolpaw et al., 2002; Birbaumer and Cohen, 2007; Daly and Wolpaw, 2008). In this decade, the use of BCI technology has become widespread, mainly for preclinical research, due to technical and mechanical improvements, and new technology been designed to help individuals with severe neurological disabilities, especially motor difficulties such as amyotrophic lateral sclerosis (ALS), spinal cord injury (SCI), and cerebral stroke.

Scalp electroencephalography (EEG)-based BCI devices are non-invasive and easy to use in daily life. Several methods have been developed for their use based on slow cortical potentials (SCP) (Birbaumer et al., 1999; Kübler et al., 1999), sensorimotor rhythms (SMR) (Pfurtscheller et al., 2000; Wolpaw and McFarland, 2004), steady-state visual evoked potentials (SSVEP) (Müller-Putz et al., 2005; Allison et al., 2008), and P300 even-related potentials (Farwell and Donchin, 1988; Sellers and Donchin, 2006). Training is needed to control SCP or SMR, and the efficacy of higher frequency bands of SMR has been reported using invasive methods (Leuthardt et al., 2004; Hochberg et al., 2006; Yanagisawa et al., 2012). In recent invasive P300 BCI studies, electrocorticographic (ECoG) electrodes were placed around the parietal and occipital lobes, allowing successful operation of the visual P300 speller (Brunner et al., 2011; Krusienski and Shih, 2011).

The P300 responses were evoked by attention to random rare stimuli (i.e., the oddball paradigm). The response was easily detected from the scalp EEG as a positive potential occurring about 300 ms after stimulus onset (Sutton et al., 1965; Polich, 2007). Farwell and Donchin (1988) used this response to develop the P300 speller, which presents a selection of icons arranged in a matrix with row or column intensification. Importantly, minimal training was required to use the P300 BCI (Donchin et al., 2000; Wolpaw et al., 2002; Kaper et al., 2004; Krusienski et al., 2006, 2008; Sellers et al., 2006; Takano et al., 2009b). Some visual P300 BCI systems that were modified from the P300 speller have already been tested with tetraplegia patients, including ALS patients (Piccione et al., 2006; Sellers and Donchin, 2006; Hoffmann et al., 2008; Kubler and Birbaumer, 2008; Nijboer et al., 2008; Silvoni et al., 2009; Ikegami et al., 2011; Kaufmann et al., 2013).

However, some difficulties with the use of conventional row/column P300 spellers have been reported. The overlap and refractory effects influence the P300 ERP components and decrease target classification accuracy (Martens et al., 2009; Townsend et al., 2010). Non-target flashes in the row or column adjacent to the attended target attract the participant's attention and may produce P300 responses (Fazel-Rezai, 2007; Townsend et al., 2010). Improvements in visual presentation are therefore required. Recently, two- (and higher)-level paradigms (including region-based, hex-o-spell or multi-menu paradigms) have been introduced (Fazel-Rezai and Abhari, 2008; Treder and Blankertz, 2010; Jarmolowska et al., 2013). Townsend et al. produced a checkerboard paradigm and demonstrated improvements in BCI performance for three ALS subjects (Townsend et al., 2010).

Our research group recently developed a visual P300 BCI system and added chromatic change to conventional luminance change in a flicker matrix. We showed that stimuli employing chromatic and luminance change for the visual P300 speller were associated with a better subjective feeling of comfort compared with the conventional luminance stimuli (Takano et al., 2009a). Moreover, we also found that the flicker matrix using both chromatic and luminance change was associated with better performance (Takano et al., 2009b). The visual P300-BCI system was also used successfully by patients with cervical spinal cord injury (Ikegami et al., 2011).

Difficulties in spelling with the P300 Speller for ALS patients have previously been reported (Sellers et al., 2003; McCane et al., 2009). These patients had a difficulty seeing the speller matrices, presumably due to decreased visual performance (e.g., ptosis, nystagmus); however, a P300-like wave was elicited from these patients in an oddball task. To account for this, a four-choice oddball paradigm was used with a previously reported initial BCI test in ALS patients (Sellers and Donchin, 2006). Another group developed their own visual P300 BCI systems and reported the successful use of the P300 speller matrix with conventional row/column intensification in individuals with ALS (Nijboer et al., 2008); in their study the mean ALS Functional Rating Scale (ALSFRS) score of the patients was 12 (range 4–20) of 40. However, the relationship between the P300 BCI performance of ALS patients and their ALSFRS scores has yet to be elucidated.

Recently, we started a BCI project that included patients with ALS. In a preliminary study, a 61-year-old ALS patient with an ALSFRS score of 0 reported that small icons on the RC speller may be difficult to see. We therefore modified the RC speller matrix using a region-based two-step procedure. We divided a 6 × 9-hiragana (Japanese character) matrix into six circled background regions including nine characters each. First, as each of these circles was intensified, the subject attended to the background circle including the target character. When the circled region was selected, the speller matrix moved to the second step. In the second step, each character was intensified within the circled background region, similar to the first step, and the subjects then selected the target character (two-step procedure).

In this study, we focused on the effectiveness of visual P300 BCI in ALS patients whose ALSFRS scores were relatively low, and who were relatively elderly, comparing their performance to that of age- and sex-matched able-bodied controls. Subjects were required to input hiragana characters using two types of input paradigm, traditional row/column (RC) and two-step conditions, using our P300 BCI with visual flicker stimuli that employed green/blue luminance changes as well as chromatic changes. By comparing the two, we showed that the modified visual P300 BCI was effective for ALS patients.

2. Methods

2.1. Subjects

Seven patients with ALS (age 59–68 years, mean 64.1 years, three men) with no prior training with BCI devices were recruited as participants (summarized in Table 1). The mean ALSFRS-revised (ALSFRS-R) (Cedarbaum and Stambler, 1997) score was 9.4 (range 0–38, median 6). The mean time since onset was 6.1 (range 2.2–16.2, median 5.3) years. Six patients had gastrostomas, and five had undergone tracheostomies. Six of the ALS patients used alternative augmentative communication (AAC) devices to communicate with others using residual muscle movement (e.g., brow twitch). One patient was an outpatient and was tested in his home environment, and the others were tested at Yoka Hospital. Seven age- and sex-matched able-bodied controls (age 58–68 years, mean 64.0 years, three men) with no prior experience with BCI devices were recruited. This study received approval from the institutional review board, and all subjects provided written informed consent according to institutional guidelines.

2.2. Visual stimuli

The conventional P300 speller was based on the visual oddball paradigm and used random intensification of each row/column to

Table 1
Summary of amyotrophic lateral sclerosis patients.

No.	Age	Sex	ALSFRS-R	Time since onset (years)	Gastrostoma	NPPV	TPPV	AAC devices
1	61	Male	0	16.2	Y	N	Y	Y
2	65	Female	0	6.2	Y	N	Y	Y
3	67	Male	1	7.2	Y	Y	Y	Y
4	68	Male	6	2.2	Y	Y	Y	Y
5	63	Female	8	5.3	Y	N	Y	Y
6	66	Female	13	2.9	Y	N	N	Y
7	59	Female	38	2.5	N	Y	N	N

AAC, augmentative and alternative communication.
ALSFRS-R, amyotrophic lateral sclerosis functional rating scale-revised.
TPPV, tracheotomy positive-pressure ventilation.
NPPV, non-invasive positive-pressure ventilation.

select one character arranged in a matrix (Farwell and Donchin, 1988). This P300 speller used a 6 × 6 matrix of icons consisting of 26 English alphabet and 10 numeric character or symbols. To input Japanese hiragana characters, we prepared a 6 × 9 matrix for the P300 speller (Fig. 1). The matrix consisted of 48 hiragana characters and four other symbols and thus had fewer items than our previous 8 × 10 matrix (Takano et al., 2009b; Ikegami et al., 2011). The traditional visual stimulus in a visual P300 BCI was a luminance change in the icons (Farwell and Donchin, 1988). Previously, we showed that the addition of a green/blue chromatic change to the luminance change improved performance on the P300 speller (Takano et al., 2009b; Ikegami et al., 2011). Therefore, we used green/blue chromatic and luminance changes in this study. The duration of intensification was 100 ms, and the rest period was 75 ms, as in previous studies (Blankertz et al., 2006; Sellers et al., 2006; Takano et al., 2009b; Ikegami et al., 2011).

We prepared two types of speller conditions. One was a standard row/column (RC) speller condition. Under the RC condition, according to the P300 speller protocol, each row/column in the matrix intensified randomly, and the participant focused on one icon as the target (Fig. 1a). One complete cycle of intensification of six rows and nine columns constituted a sequence (two target stimuli and 13 non-target stimuli). The target stimuli were presented as rare stimuli (i.e., the oddball paradigm) and elicited P300 responses, whereas the other non-target rows and columns did not. During a sequence, we recorded and analyzed EEG data online, and the intersection of the classified row and column was regarded as the target.

The other condition used a two-step process (two-step condition), which was modified from previous reports (Fazel-Rezai, 2007; Treder and Blankertz, 2010). We divided the 6 × 9 matrix into six circled regions including nine characters each. First, each region was individually intensified, and the subject attended to the background circle that included the target character. When the region was selected, the speller matrix moved to the second step (Fig. 1b). In the second step, each character was intensified within the circled background region, similar to the first step, and the subjects then selected the target character. The first step used 2 × 3 regions, and the second step used 3 × 3 regions. The bottom row was empty in the first step. Thus, if in practice, a user requested a function (e.g., a button to return to the top level for an error correction), the icons could be included there. Under this condition, the circles intensified one by one in random order. One complete intensification cycle of six regions for the first step and nine regions for the second step constituted a sequence (one target stimulus and five non-target stimuli in the first step, one target stimulus and eight non-target stimuli in the second step).

Each letter (or circle) was selected in a series of eight sequences (one trial), including 120 intensifications for each hiragana character in the RC condition and 48 (first step) + 72 (second step) circle intensifications in the two-step condition. The intensification duration was set identically for both conditions; however, because of classification intervals for first step, the time required to input one letter was longer in the two-step condition than in the RC condition.

2.3. EEG recording and analysis

Eight-channel (Fz, Cz, Pz, P3, P4, Oz, PO7, and PO8; Krusienski et al., 2008; Takano et al., 2009b; Ikegami et al., 2012) EEG data were recorded with an in-house cap and an in-house amplifier (Toyama et al., 2012). EEG signals were band-pass filtered (0.1–50 Hz), digitized at 1024 Hz, and stored. All channels were referenced to Fpz and grounded to AFz. Recorded EEG data were downsampled to 21 Hz for analysis. A total of 800 ms of EEG data were segmented according to the timing of flash onset. The first 100-ms period, occurring just prior to flash onset, was used for baseline correction, and the remaining 700 ms was used for classification. In the training session, feature vectors were derived for each condition (RC and two-step). During the test session, using these feature vectors, target and non-target characters were discriminated using Fisher's linear discriminant analysis. The result of this classification, the maximum of the summed scores, was used to determine the icon or circle to which the subjects were attending. Under the RC condition, the intersection of the calculated row and column was regarded as the target.

2.4. Procedure

Six of seven ALS subjects lay supine on a bed because of their clinical condition. A liquid crystal display (LCD) that displayed visual stimuli and an input window was set approximately 100 cm away from their face using a flexible monitor arm. Another ALS subject and all control subjects sat in a desk chair approximately 100 cm away from a standard LCD monitor. We first collected EEG data to derive feature vectors for a subsequent spelling session. Under the RC condition, subjects were instructed to attend to six successive icons to derive the feature vectors. Under the two-step condition, we used the 3 × 3 matrix of the second step and subjects were instructed to attend to nine regions sequentially to derive the feature vectors. Thus, fewer data were collected for the classifier under two-step conditions than under RC conditions. During a trial, all subjects were instructed to attend to a target letter. In the spelling session, all subjects were required to input six successive characters (six trials) under each speller condition. The percentage of characters entered correctly was defined as the classification accuracy. The order of the experimental conditions (RC or two-step) was randomized among subjects. The aim of this project was to apply BCIs for patients with ALS as a possible alternative method of communication. No ALS subject

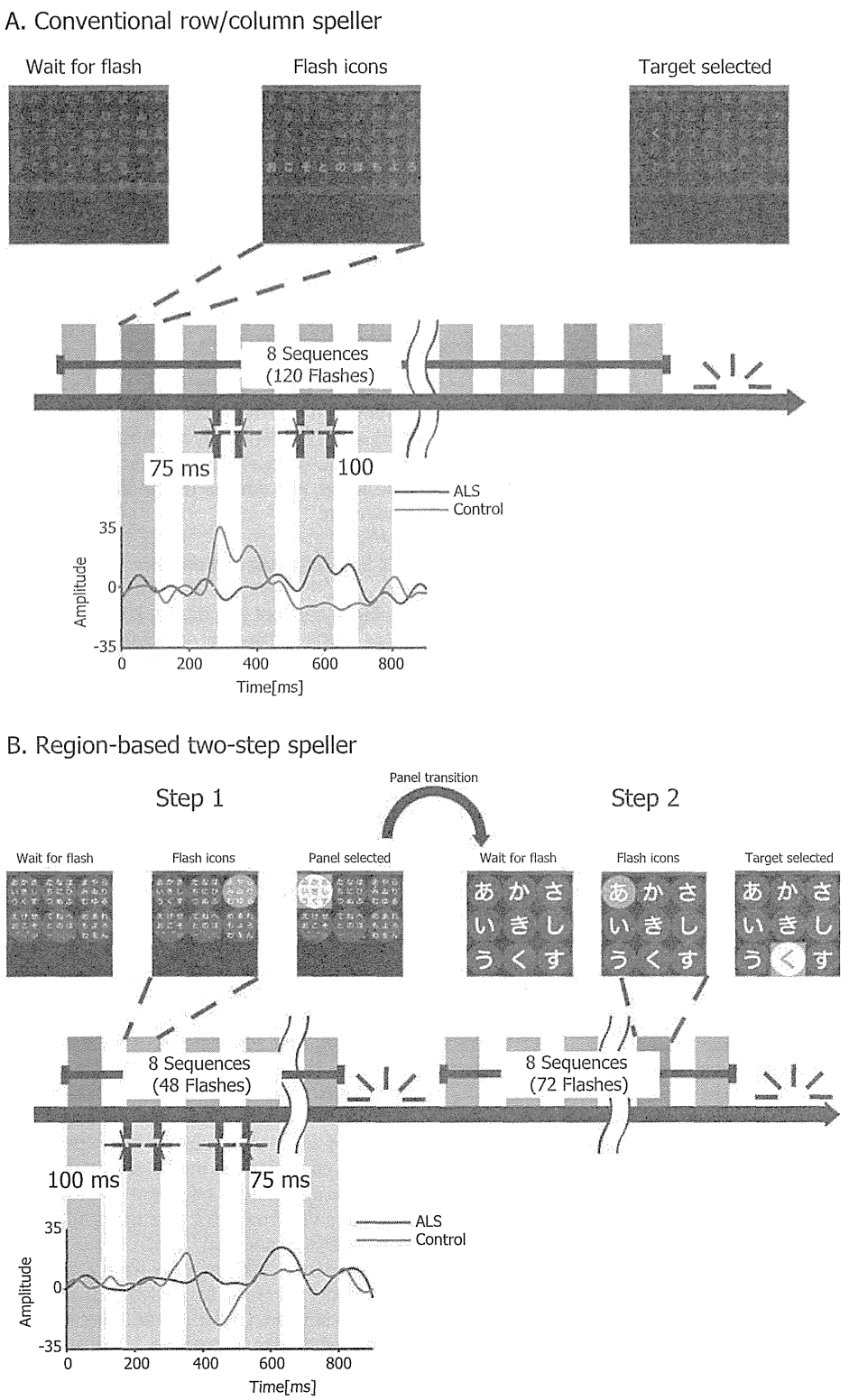

Fig. 1. Task timing for two types of hiragana speller paradigms: (A) a conventional row/column (RC) speller and (B) a region-based two-step speller. The stimulus onset asynchrony was 175 ms, including 100 ms of intensification and 75 ms of rest. EEG data were collected and used for classification over eight sequences. Representative ERP waves of a subject from each group in response to a target stimulus are shown at the bottom of (A) and (B).

had better accuracy under RC conditions than under the two-step conditions in the first experiment. Therefore, we provided additional experience using our P300-BCI system approximately once every 2 months for 1 year to those ALS subjects whose performance was not sufficient for practical use, defined as >70% accuracy (Sellers et al., 2006; Kubler and Birbaumer, 2008; Nijboer et al., 2008), but was enhanced with the new speller in the first experiment. Then, we evaluated the performance of the P300-BCI speller under the two-step condition after 1 year of additional use.

We evaluated the online performance for ALS and control subjects under each RC and two-step condition. Correlations between ALS subjects' accuracy and their demographic characteristics (age,

time since onset, ALSFRS-R score) were evaluated using Spearman's rank correlation coefficient. Because the sample size was too small for parametric statistics, we used the Kruskal–Wallis test to compare the online accuracy of the groups (ALS vs. control) under each condition and the conditions (RC vs. two-step) for each group.

3. Results

3.1. Online performance

All subjects completed the six-letter spelling task under both the RC and two-step conditions. The mean online accuracy of all subjects was 47.6% for the RC condition and 69.0% for the two-step condition. Under the RC condition, the mean accuracy was 71.4% for the control group and 23.8% for the ALS group. Under the two-step condition, the mean accuracy was 83.3% and 54.8% for control and ALS groups, respectively (Fig. 2).

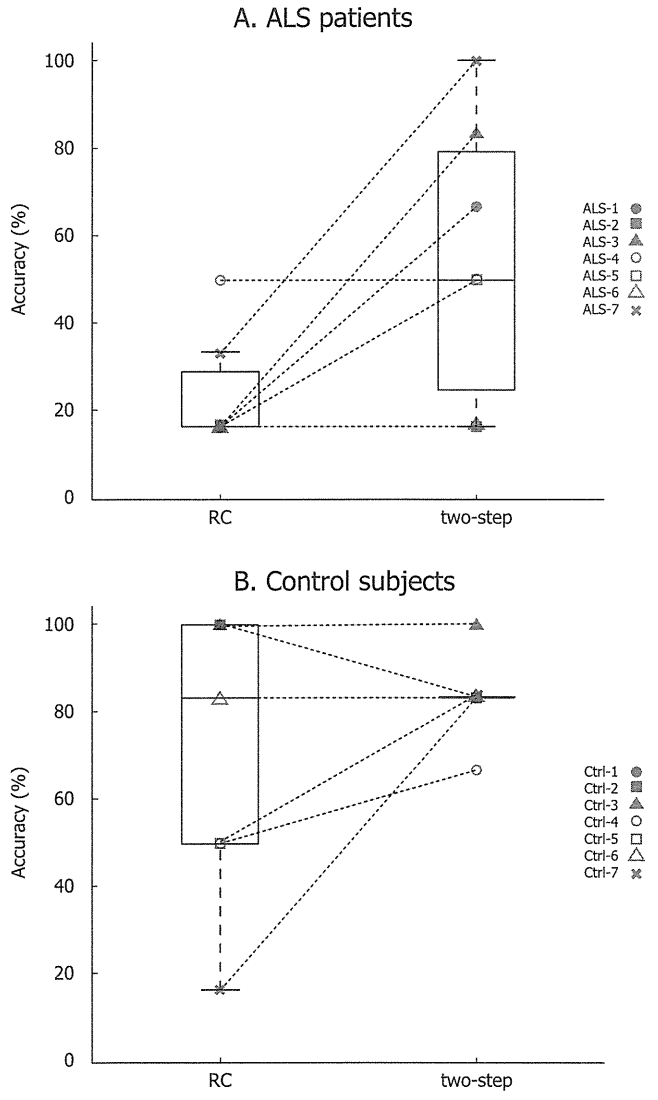

Fig. 2. Online accuracy of each (A) ALS patient and (B) control subject for each condition (RC and two-step) was plotted with a box plot. The central red line represents the median, the edges of the box are the 25th and 75th percentiles, and the whiskers extend to the most extreme data points. The two-step condition resulted in better accuracies than the RC condition among ALS patients, and a significant difference was shown between the two conditions (paired *t*-test, $p < 0.05$).

The Kruskal–Wallis test revealed a significant difference between ALS and control subjects under RC conditions [$\chi^2(1) = 6.51$, $p = 0.011$] but not under the two-step conditions [$\chi^2(1) = 3.50$, $p = 0.061$]. Importantly, the accuracy of ALS subjects improved significantly under two-step conditions compared with RC conditions [$\chi^2(1) = 3.95$, $p = 0.047$]. However, these effects were not significant in control subjects.

No significant correlations were observed between accuracy under two-step conditions and demographic characteristics (age, time since onset, and ALSFRS-R score). However, a significant correlation was found between accuracy under the RC condition and the time since onset (Spearman's rank correlation coefficient, $p < 0.05$). Two of seven ALS subjects (ages 61 and 63, a male and a female) participated in subsequent experiment using the two-step paradigm (approximately once every 2 months), and their mean accuracy increased to 92% (100% and 83%; Table 2). Therefore, four ALS patients in total, including these two subjects, successfully controlled the region-based two-step speller (i.e., >70% correct (Sellers and Donchin, 2006; Kubler and Birbaumer, 2008; Nijboer et al., 2008)).

3.2. Errors in both paradigms

Fig. 3 lists the number of errors relative to the target characters for both groups under the RC condition (Fazel-Rezai, 2007; Townsend et al., 2010). Numbers outside the box show distances from the target characters (asterisk in the center of the shaded area). Eighty-one percent of all errors of the ALS group occurred in the same row or column (the shaded area). This result was similar to the previous data from able-bodied (Fazel-Rezai, 2007; Townsend et al., 2010) and from our control subjects (Fig. 3, below). Under the two-step condition, the error rate was 21% for the first step (six choices) and 40% for the second step (nine choices); this difference was not significant (Table 3). The accuracy at each step was similar to accuracies reported in the previous studies.

4. Discussion

We investigated the visual P300-based BCI performance in individuals with amyotrophic lateral sclerosis using two types of visual P300 speller. ALS patients controlled our P300 BCI system, and the two-step procedure provided higher accuracy at each step than the conventional RC speller, as well as age- and sex- matched control subjects.

4.1. BCI performance in ALS patients

Previous studies had described the offline and online BCI performance of ALS subjects (summarized in Tables 2 and 3; Piccione et al., 2006; Sellers and Donchin, 2006; Hoffmann et al., 2008; Nijboer et al., 2008; Silvoni et al., 2009; Townsend et al., 2010; Kaufmann et al., 2013). Our ALS subjects had relatively low ALSFRS-R scores (range 0–38; median 6), and six of the seven patients remained in bed for most of the day due to their clinical condition. Although most of the subjects in previous BCI studies were tested in a sitting position, for these subjects, we presented the visual stimuli via a LCD monitor fixed by a flexible arm as they lay in a supine position. In previous reports, the physical impairments of ALS patients did not affect P300 BCI performance (Kubler and Birbaumer, 2008; Nijboer et al., 2008), nor was the BCI performance influenced by disease progression (Silvoni et al., 2009). Kubler and Birbaumer (2008) reviewed previous reports of BCI performance in disabled subjects and investigated the relationship

Table 2
Online P300-BCI speller performance.

No. of subjects	Age (mean)	ALSFRS-R (mean)	Level of impairment[a]	Speller type	No. of choices	Mean accuracy (%)	Reference
8	36–67 (48.5)	6–17[b] (12.3)	2–4	RC	36[c] 36/49[d]	62 80	Nijboer et al. (2008)
3	N.A.	N.A.	4	RC CB	72	45–70[e] 75–89[e]	Townsend et al. (2010)
4	48–51 (54.3)	N.A.	1–3	RC	36	55[f] 100[g]	Kaufmann et al. (2013)
7	59–68v(64.1)	0–38 (9.4)	2–4	RC two step	54	24 55 92[h]	Present study

RC = row/column speller; CB = checkerboard speller; N.A. = data not available
[a] Kubler and Birbaumer (2008).
[b] ALSFRS-R.
[c] Six of eight patients.
[d] Three of eight patients.
[e] Data estimated from figure.
[f] Classic character flashing.
[g] Famous face flashing.
[h] Two of seven patients after additional experience.

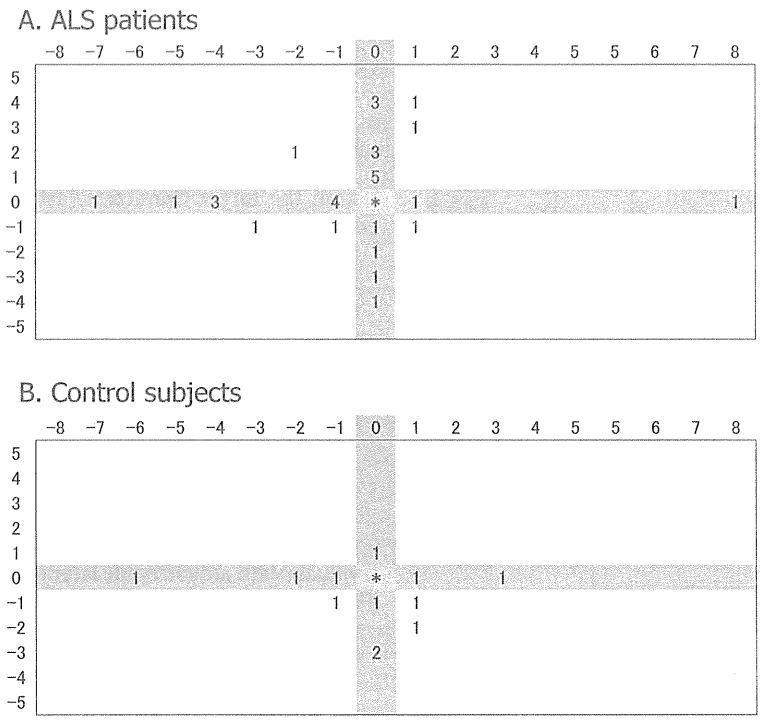

Fig. 3. Errors occurred in the RC condition for ALS subjects (A) and for control subjects (B). The number of errors relative to the target characters for ALS and control subjects under the RC condition is shown in each box. Numbers outside the table indicate distance from the target characters (asterisk at the center of the shaded area). The errors among ALS and control subjects had similar distributions.

Table 3
Performance of single icon flickering matrix P300-BCI for ALS patients.

No. of subjects	Age (mean)	ALSFRS-R (mean)	Level of impairment[a]	No. of choices	Mean accuracy (%)	Online/offline	Published in
3	37–50 (43.7)	N.A.	2–3	4	72	Offline	Sellers and Donchin (2006)
1	75	N.A.	3	4	80	Offline	Piccione et al. (2006)
1	47	N.A.	3	6	100	Offline	Hoffmann et al. (2008)
21	29–73 (55.6)	19–43 (32.2)	1–3	4	79	Online	Silvoni et al. (2009)
7	59–68 (64.1)	0–38 (9.4)	2–4	6	79	Online	Present study
				9	60		

N.A. = data not shown.
[a] Kubler and Birbaumer (2008).

between performance and physical impairment. With the exception of patients with complete locked-in syndrome (CLIS), they found no correlation between level of impairment and performance; however, when CLIS patients were included, a strong correlation was detected. We included two patients whose ALSFRS-R score was 0 in our subjects, and our results showed no correlation between ALSFRS-R and P300 BCI performance.

The mean age of our ALS subjects was 64.1 (range 59–68) years. Aging is known to influence P300 (Picton et al., 1984; Friedman et al., 1997; Fjell and Walhovd, 2001) and color perception (Suzuki et al., 2006), and the BCI performance of our control subjects (age 58–68 years, mean 64.0 years) was similar to previous results (Takano et al., 2009b; Ikegami et al., 2011). Although Silvoni et al. (2009) reported that aging influenced BCI performance in ALS patients, we saw no age differences in the BCI performance of our ALS patients. The mean time since onset in our ALS subjects was 6.1 (range 2.2–16.2) years. Our results showed that the duration of disease was associated with decreased RC speller performance.

For ALS patients, the two-step procedure provided significantly increased accuracy compared with a conventional RC speller. Furthermore, the accuracy was significantly lower in the ALS patients than in the control subjects under the RC condition, although the new visual stimuli significantly increased accuracy in these patients. Using the new speller, two ALS patients showed initial accuracy sufficient for practical use (>70%); two other ALS patients who performed better using the new speller in the first trial participated further, and their mean accuracies increased to 92%. The extended experience was required to train subjects as well as their caregivers, especially in preparation and cleanup (Zickler et al., 2011). The ALS patients showed increased accuracy following the extended BCI experience. We feel that it took time to become familiar with the BCI system, and we suggest that it may be beneficial to introduce the system to candidates as early as possible (Birbaumer, 2006; Kubler and Birbaumer, 2008).

4.2. Effect of visual stimuli in the P300 speller

In the conventional row/column P300 speller paradigm, each row and column is intensified randomly, and the overlap and refractory effects (Martens et al., 2009), double flash errors (Townsend et al., 2010) or errors of the non-target icons adjacent to attended target (Fazel-Rezai, 2007; Townsend et al., 2010) have been reported. These errors decrease the accuracy of target classification. Errors in the same row and column of the attended target (Fazel-Rezai, 2007; Townsend et al., 2010) were observed in ALS patients as well as control subjects (see Fig. 3). This error occurred because of subjects' attention to the non-target adjacent to the target (Townsend et al., 2010).

To reduce these types of errors, two-step paradigms such as region-based (Fazel-Rezai and Abhari, 2008) or hex-o-spell (Treder and Blankertz, 2010) paradigms have been introduced, and improvement in BCI performance compared with conventional RC paradigms has been reported among able-bodied subjects. One of these paradigms, a checkerboard paradigm was tested in three ALS patients. Using this approach, Townsend et al. reported the successful use of their BCI (Townsend et al., 2010). Recently, Kaufmann et al. proposed a face-flashing (FF) paradigm for the RC P300 speller, in which each row and column were simply highlighted with well-known faces (Kaufmann et al., 2013). Importantly, the FF paradigm significantly improved spelling performance compared with the conventional RC speller in both able-bodied and disabled subjects. This simple modification of visual presentation for P300 BCI may therefore be effective to avoid these types of errors. In the present study, the mean accuracy of our relatively elderly ALS subjects with low ALSFRS scores was significantly higher under two-step than under RC conditions. The visual presentation in the two-step paradigm was more easily discriminated by our ALS patients, suggesting that these visual stimuli may enhance P300 performance due to their relatively ease of visualization (Polich, 1987; Ikegami et al., 2012).

Guger et al. (2009) reported that able-bodied subjects achieve higher accuracy on their P300 BCI system with the 6×6 matrix using an RC paradigm than with a single-character paradigm that flashed each character individually. Sellers and Donchin (2006) choose the single-character paradigm with four choices in their initial BCI test with ALS patients and reported a mean performance rate of 72% (see Table 3). Jarmolowska et al. (2013) reported a "multi-menu" system that arranged a small matrix of words. The 3×3 multi-menu used in their study enabled faster communication than conventional RC spellers while providing the same level of accuracy as the 6×6 matrices. In the present study, the mean accuracy was higher under the two-step condition than under the RC condition among ALS subjects. Under the two-step condition, the accuracy for the first step (six choices) was 79%, and that for the second step (nine choices) was 60. When using a single-character paradigm for the P300 speller the lower number of choices resulted in increased accuracy in ALS patients. Some ALS patients had ptosis and were easily fatigued. It has been reported that the gaze control of the operators affects their BCI performance (Brunner et al., 2010; Treder and Blankertz, 2010). Therefore, the relatively low performance of ALS patients may be partly explained by their gaze control.

We have been developing BCI for ALS patients as a potential alternative communication option. For the practical use of P300 BCI, accurate and fast communications with ease of use are required (Zickler et al., 2011). This study demonstrated that the two-step speller improved the P300 BCI performance of the ALS patients. Furthermore, we are currently developing a BCI system that includes non-adhesive solid-gel electrodes for easier use (Toyama et al., 2012). A rapid communication speller incorporating such electrodes would contribute to the practical utility of P300 BCI.

In summary, this study developed a region-based two-step procedure for a visual P300-based BCI hiragana speller for ALS patients. The two-step speller may be beneficial for some ALS patients who are not skilled at using conventional RC spellers. The extended experience resulted in improved performance, although additional studies are required to aid the development of a practical BCI that will allow these individuals to expand their range of activities.

Acknowledgments

This study was partially supported by a Grant-in-Aid from the Ministry of Health, Labor and Welfare of Japan to K.K. We thank Drs. T. Komatsu, N. Nagao, M. Yoneda, and T. Togaki for their help and Dr. Y. Nakajima for his continuous encouragement.

References

Allison BZ, McFarland DJ, Schalk G, Zheng SD, Jackson MM, Wolpaw JR. Towards an independent brain-computer interface using steady state visual evoked potentials. Clin Neurophysiol 2008;119:399–408.
Birbaumer N. Breaking the silence: brain-computer interfaces (BCI) for communication and motor control. Psychophysiology 2006;43:517–32.
Birbaumer N, Cohen LG. Brain-computer interfaces: communication and restoration of movement in paralysis. J Physiol 2007;579:621–36.
Birbaumer N, Ghanayim N, Hinterberger T, Iversen I, Kotchoubey B, Kübler A, et al. A spelling device for the paralysed. Nature 1999;398:297–8.
Blankertz B, Muller KR, Krusienski DJ, Schalk G, Wolpaw JR, Schlogl A, et al. The BCI competition. III: validating alternative approaches to actual BCI problems. IEEE Trans Neural Syst Rehabil Eng 2006;14:153–9.
Brunner P, Joshi S, Briskin S, Wolpaw JR, Bischof H, Schalk G. Does the 'P300' speller depend on eye gaze? J Neural Eng 2010;7:056013.
Brunner P, Ritaccio AL, Emrich JF, Bischof H, Schalk G. Rapid communication with a "P300" matrix speller using electrocorticographic signals (ECoG). Front Neurosci 2011;5:5.

Cedarbaum JM, Stambler N. Performance of the amyotrophic lateral sclerosis functional rating scale (ALSFRS) in multicenter clinical trials. J Neurol Sci 1997;152(Suppl 1):S1–9.
Daly JJ, Wolpaw JR. Brain–computer interfaces in neurological rehabilitation. Lancet Neurol 2008;7:1032–43.
Donchin E, Spencer KM, Wijesinghe R. The mental prosthesis: assessing the speed of a P300-based brain–computer interface. IEEE Trans Rehabil Eng 2000;8:174–9.
Farwell LA, Donchin E. Talking off the top of your head: toward a mental prosthesis utilizing event-related brain potentials. Electroencephalogr Clin Neurophysiol 1988;70:510–23.
Fazel-Rezai R. Human error in P300 speller paradigm for brain–computer interface. Conf Proc IEEE Eng Med Biol Soc 2007;2007:2516–9.
Fazel-Rezai R, Abhari K. A comparison between a matrix-based and a region-based P300 speller paradigms for brain–computer interface. Conf Proc IEEE Eng Med Biol Soc 2008;2008:1147–50.
Fjell AM, Walhovd KB. P300 and neuropsychological tests as measures of aging: scalp topography and cognitive changes. Brain Topogr 2001;14:25–40.
Friedman D, Kazmerski V, Fabiani M. An overview of age-related changes in the scalp distribution of P3b. Electroencephalogr Clin Neurophysiol 1997;104: 498–513.
Guger C, Daban S, Sellers E, Holzner C, Krausz G, Carabalona R, et al. How many people are able to control a P300-based brain–computer interface (BCI)? Neurosci Lett 2009;462:94–8.
Hochberg LR, Serruya MD, Friehs GM, Mukand JA, Saleh M, Caplan AH, et al. Neuronal ensemble control of prosthetic devices by a human with tetraplegia. Nature 2006;442:164–71.
Hoffmann U, Vesin JM, Ebrahimi T, Diserens K. An efficient P300-based brain–computer interface for disabled subjects. J Neurosci Methods 2008;167:115–25.
Ikegami S, Takano K, Saeki N, Kansaku K. Operation of a P300-based brain–computer interface by individuals with cervical spinal cord injury. Clin Neurophysiol 2011;122:991–6.
Ikegami S, Takano K, Wada M, Saeki N, Kansaku K. Effect of the green/blue flicker matrix for P300-based brain–computer interface: an EEG-fMRI Study. Front Neurol 2012;3:113.
Jarmolowska J, Turconi MM, Busan P, Mei J, Battaglini PP. A multimenu system based on the P300 component as a time saving procedure for communication with a brain-computer interface. Front Neurosci 2013;7:39.
Kaper M, Meinicke P, Grossekathoefer U, Lingner T, Ritter H. BCI Competition 2003 – Data set IIb: support vector machines for the P300 speller paradigm. IEEE Trans Biomed Eng 2004;51:1073–6.
Kaufmann T, Schulz SM, Koblitz A, Renner G, Wessig C, Kubler A. Face stimuli effectively prevent brain–computer interface inefficiency in patients with neurodegenerative disease. Clin Neurophysiol 2013;124:893–900.
Krusienski DJ, Shih JJ. Control of a visual keyboard using an electrocorticographic brain–computer interface. Neurorehabil Neural Repair 2011;25:323–31.
Krusienski DJ, Sellers EW, Cabestaing F, Bayoudh S, McFarland DJ, Vaughan TM, et al. A comparison of classification techniques for the P300 Speller. J Neural Eng 2006;3:299–305.
Krusienski DJ, Sellers EW, McFarland DJ, Vaughan TM, Wolpaw JR. Toward enhanced P300 speller performance. J Neurosci Methods 2008;167:15–21.
Kubler A, Birbaumer N. Brain–computer interfaces and communication in paralysis: extinction of goal directed thinking in completely paralysed patients? Clin Neurophysiol 2008;119:2658–66.
Kübler A, Kotchoubey B, Hinterberger T, Ghanayim N, Perelmouter J, Schauer M, et al. The thought translation device: a neurophysiological approach to communication in total motor paralysis. Exp Brain Res 1999;124:223–32.
Leuthardt EC, Schalk G, Wolpaw JR, Ojemann JG, Moran DW. A brain–computer interface using electrocorticographic signals in humans. J Neural Eng 2004;1: 63–71.
Martens SM, Hill NJ, Farquhar J, Scholkopf B. Overlap and refractory effects in a brain–computer interface speller based on the visual P300 event-related potential. J Neural Eng 2009;6:026003.
McCane L, Vaughan TM, McFarland DJ, Zeitlin D, Tenteromano L, Mak J, et al. Evaluation of Individuals with ALS for in home use of a P300 brain–computer interface. In: Program No 6647 2009 neuroscience meeting planner Chicago, IL: Society for Neuroscience, 2009 Online. 2009.
Müller-Putz GR, Scherer R, Brauneis C, Pfurtscheller G. Steady-state visual evoked potential (SSVEP)-based communication: impact of harmonic frequency components. J Neural Eng 2005;2:123–30.
Nijboer F, Sellers EW, Mellinger J, Jordan MA, Matuz T, Furdea A, et al. A P300-based brain–computer interface for people with amyotrophic lateral sclerosis. Clin Neurophysiol 2008;119:1909–16.
Pfurtscheller G, Guger C, Müller G, Krausz G, Neuper C. Brain oscillations control hand orthosis in a tetraplegic. Neurosci Lett 2000;292:211–4.
Piccione F, Giorgi F, Tonin P, Priftis K, Giove S, Silvoni S, et al. P300-based brain–computer interface: reliability and performance in healthy and paralysed participants. Clin Neurophysiol 2006;117:531–7.
Picton TW, Stuss DT, Champagne SC, Nelson RF. The effects of age on human event-related potentials. Psychophysiology 1984;21:312–25.
Polich J. Task difficulty, probability, and inter-stimulus interval as determinants of P300 from auditory stimuli. Electroencephalogr Clin Neurophysiol 1987;68: 311–20.
Polich J. Updating P300: an integrative theory of P3a and P3b. Clin Neurophysiol 2007;118:2128–48.
Sellers EW, Donchin E. A P300-based brain–computer interface: initial tests by ALS patients. Clin Neurophysiol 2006;117:538–48.
Sellers E, Schalk G, Donchin E. The P300 as a typing tool: tests of brain–computer interface with an ALS patient. In: The 43rd annual meeting of the society for psychophysiological research. Chicago, IL; 2003.
Sellers EW, Krusienski DJ, McFarland DJ, Vaughan TM, Wolpaw JR. A P300 event-related potential brain–computer interface (BCI): the effects of matrix size and inter-stimulus interval on performance. Biol Psychol 2006;73:242–52.
Silvoni S, Volpato C, Cavinato M, Marchetti M, Priftis K, Merico A, et al. P300-based brain–computer interface communication: evaluation and follow-up in amyotrophic lateral sclerosis. Front Neurosci 2009;3:60.
Sutton S, Braren M, Zubin J, John ER. Evoked-potential correlates of stimulus uncertainty. Science 1965;150:1187–8.
Suzuki TA, Qiang Y, Sakuragawa S, Tamura H, Okajima K. Age-related changes of reaction time and p300 for low-contrast color stimuli: effects of yellowing of the aging human lens. J Physiol Anthropol 2006;25:179–87.
Takano K, Ikegami S, Komatsu T, Kansaku K. Green/blue flicker matrices for the P300 BCI improve the subjective feeling of comfort. Neurosci Res 2009a;65:S182.
Takano K, Komatsu T, Hata N, Nakajima Y, Kansaku K. Visual stimuli for the P300 brain–computer interface: a comparison of white/gray and green/blue flicker matrices. Clin Neurophysiol 2009b;120:1562–6.
Townsend G, LaPallo BK, Boulay CB, Krusienski DJ, Frye GE, Hauser CK, et al. A novel P300-based brain–computer interface stimulus presentation paradigm: moving beyond rows and columns. Clin Neurophysiol 2010;121:1109–20.
Toyama S, Takano K, Kansaku K. A non-adhesive solid-gel electrode for a non-invasive brain–machine interface. Front Neurol 2012;3:114.
Treder MS, Blankertz B. (C)overt attention and visual speller design in an ERP-based brain–computer interface. Behav Brain Funct 2010;6:28.
Wolpaw JR, McFarland DJ. Control of a two-dimensional movement signal by a noninvasive brain–computer interface in humans. Proc Natl Acad Sci USA 2004;101:17849–54.
Wolpaw JR, Birbaumer N, McFarland DJ, Pfurtscheller G, Vaughan TM. Brain–computer interfaces for communication and control. Clin Neurophysiol 2002;113:767–91.
Yanagisawa T, Hirata M, Saitoh Y, Kishima H, Matsushita K, Goto T, et al. Electrocorticographic control of a prosthetic arm in paralyzed patients. Ann Neurol 2012;71:353–61.
Zickler C, Riccio A, Leotta F, Hillian-Tress S, Halder S, Holz E, et al. A brain–computer interface as input channel for a standard assistive technology software. Clin EEG Neurosci 2011;42:236–44.

frontiers in NEUROLOGY

ORIGINAL RESEARCH ARTICLE
published: 15 May 2014
doi: 10.3389/fneur.2014.00074

Coherent activity in bilateral parieto-occipital cortices during P300-BCI operation

Kouji Takano[1], Hiroki Ora[1], Kensuke Sekihara[2], Sunao Iwaki[3] and Kenji Kansaku[1,4]*

[1] *Systems Neuroscience Section, Department of Rehabilitation for Brain Functions, Research Institute of National Rehabilitation Center for Persons with Disabilities, Tokorozawa, Japan*
[2] *Department of Systems Design and Engineering, Tokyo Metropolitan University, Tokyo, Japan*
[3] *Cognition and Action Research Group, Human Technology Research Institute, National Institute of Advanced Industrial Science and Technology (AIST), Tsukuba, Japan*
[4] *Brain Science Inspired Life Support Research Center, The University of Electro-Communications, Tokyo, Japan*

Edited by:
José Del R. Millán, Ecole Polytechnique Fédérale de Lausanne, Switzerland

Reviewed by:
N. Ramsey, University Medical Center Utrecht, Netherlands
Matthias Treder, Medical Research Council, UK

***Correspondence:**
Kenji Kansaku, Systems Neuroscience Section, Department of Rehabilitation for Brain Functions, Research Institute of National Rehabilitation Center for Persons with Disabilities, Namiki 4-1, Tokorozawa, Japan
e-mail: kansaku-kenji@rehab.go.jp

The visual P300 brain–computer interface (BCI), a popular system for electroencephalography (EEG)-based BCI, uses the P300 event-related potential to select an icon arranged in a flicker matrix. In earlier studies, we used green/blue (GB) luminance and chromatic changes in the P300-BCI system and reported that this luminance and chromatic flicker matrix was associated with better performance and greater subject comfort compared with the conventional white/gray (WG) luminance flicker matrix. To highlight areas involved in improved P300-BCI performance, we used simultaneous EEG–fMRI recordings and showed enhanced activities in bilateral and right lateralized parieto-occipital areas. Here, to capture coherent activities of the areas during P300-BCI, we collected whole-head 306-channel magnetoencephalography data. When comparing functional connectivity between the right and left parieto-occipital channels, significantly greater functional connectivity in the alpha band was observed under the GB flicker matrix condition than under the WG flicker matrix condition. Current sources were estimated with a narrow-band adaptive spatial filter, and mean imaginary coherence was computed in the alpha band. Significantly greater coherence was observed in the right posterior parietal cortex under the GB than under the WG condition. Re-analysis of previous EEG-based P300-BCI data showed significant correlations between the power of the coherence of the bilateral parieto-occipital cortices and their performance accuracy. These results suggest that coherent activity in the bilateral parieto-occipital cortices plays a significant role in effectively driving the P300-BCI.

Keywords: BMI, magnetoencephalography, imaginary coherence, P300 speller, chromatic stimuli

INTRODUCTION

The brain–machine interface (BMI) or brain–computer interface (BCI) is an interface technology that uses neurophysiological signals from the brain to control external machines or computers (1–3). Electroencephalography (EEG), in which neurophysiological signals are recorded using electrodes placed on the scalp, represents the primary non-invasive methodology for studying BMI.

Our group has used EEG and developed a BMI-based system for environmental control and communication (4). In our system, we modified a P300 speller (5). The P300 speller uses the oddball paradigm and involves the presentation of a selection of icons arranged in a matrix. According to this protocol, the participant focuses on one icon in the matrix as the target, and each row/column or individual icon in the matrix is then intensified in a random sequence. The targets are presented as rare stimuli (i.e., the oddball paradigm). We elicited P300 responses to the target stimuli and then extracted and classified these responses with respect to the target.

We prepared a green/blue (GB) flicker matrix because this color combination was considered the safest in a photosensitive epilepsy study (6). We showed that the GB flicker matrix was associated with a better subjective feeling of comfort than was the white/gray (WG) flicker matrix, and we also found that the GB flicker matrix was associated with better performance (7, 8). The BMI system was used satisfactorily by individuals with cervical spinal cord injury (9, 10).

To highlight areas involved in improving P300-BCI performance, we used simultaneous EEG–fMRI recordings; that is, we sought to identify brain areas that showed greater enhancement in the GB flicker matrix than in the WG flicker matrix. The P300 in the EEG data was detected under both conditions, and the peak amplitudes were larger at the parietal and occipital electrodes, particularly in the late components, under the GB condition than under the WG condition. fMRI data showed activation in the bilateral parietal and occipital cortices, and these areas, particularly those in the right hemisphere, were more activated under the GB condition than under the WG condition. The parietal and occipital regions more involved under the GB condition were among the areas involved in conventional P300s, suggesting the importance of the parietal and occipital regions, especially in the right hemisphere, for the operation of P300-BCI with the GB flicker matrix (11).

Our fMRI–EEG study suggested the importance of the parietal and occipital regions, especially in the right hemisphere, for the operation of P300-BCI with the GB flicker matrix. Analysis of

coherence between these regions was expected to show how these regions cooperate in enhancing task performance (12). However, we did not conduct a detailed investigation of coherent activity in these areas because the EEG data were recorded from 27 channels, and the data included severe artifacts due to fMRI scanning. Thus, it was difficult to investigate coherent regional activity in detail.

In this study, we used 306-channel whole-head magnetoencephalography (MEG), which has high spatial resolution compared with EEG, to investigate coherent activity in these areas during the P300-BCI operation. In the coherence analysis, we specifically focused on the alpha band because it has been suggested to be involved in attentional mechanisms (13, 14). In fact, alpha-band oscillation is relevant to visual attention (15–17). Treder and colleagues showed that the alpha power of EEG signals (Po3, Po4) during eye closing in a session before BCI operation was positively correlated with the accuracy of the BCI operation (18). Furthermore, a meaningful shape induces greater alpha-band coherence than a meaningless shape (19).

To capture the coherent activities, we first applied sensor-based analysis. The sensor position and angle can be rearranged for a virtual sensor. We further used a narrow-band adaptive spatial filter to transform the sensor to voxels. We used the imaginary coherence of MEG signals between voxels to investigate functional connectivity when the P300 speller was used. Imaginary coherence uses the imaginary part of the coherence between the channels or between the voxels. It can remove spurious results due to leakage of the imaging algorithm, and thus gives more accurate results without blur (20–22). In recent clinical studies, imaginary coherence was utilized in the preoperative MEG evaluation (23, 24), and these studies have suggested the biological significance of imaginary coherence for evaluating functional connectivity. To highlight brain area(s) that may help improve P300-BCI accuracy, we used mean imaginary coherence (MIC) (25). In our previous EEG–fMRI study, we showed that greater activity was elicited in the right inferior parietal lobule by GB than by WG flicker (11). Based on that study, here, we defined a spherical region of interest (ROI) at the coordinates in the parietal area.

Finally, we reanalyzed some previous EEG-based P300-BCI data, and further investigated the coherence of the power spectrum between bilateral parieto-occipital cortices and performance accuracy.

MATERIALS AND METHODS

SUBJECTS

Thirteen healthy subjects (mean age: 22.9 years, all men, right-handed) participated. One subject's data were rejected because of excessive noise. All subjects were neurologically normal and right-handed according to the Edinburgh Inventory.

This study received approval from the Institutional Review Board at the National Rehabilitation Center for Persons with Disabilities, Tokorozawa, Japan. All subjects provided written informed consent according to institutional guidelines.

TASK

During the experiment, each participant sat on a chair. Visual stimuli were projected on a screen located in front of participants. The stimulus and triggers that indicated the onset of each trial were presented using Presentation (Neurobehavioral Systems, Inc., Albany, CA, USA).

We used two types (GB luminance chromatic condition and WG luminance condition) of visual-flicker stimuli in a 6×6 alphabet flicker matrix, modified from the "P300 speller" (5). We prepared a white (20 cd/cm)/gray (6.5 cd/cm) matrix for the WG condition, and a green (20 cd/cm)/blue (6.5 cd/cm) matrix for the GB condition; the luminance was measured using a chromatic meter (CS-200, Konica Minolta Sensing, Inc., Osaka, Japan) on the computer screen, as in our previous study (11). That is, the same luminance change was used under both GB and WG conditions as in the study. We used 100 ms of intensification and 100 ms of rest, because recent visual P300-BCI studies have usually used about 125–300 ms for stimulus-onset asynchrony (SOA) to facilitate rapid communication. Each row/column of the matrix was intensified in random order (**Figure 1**).

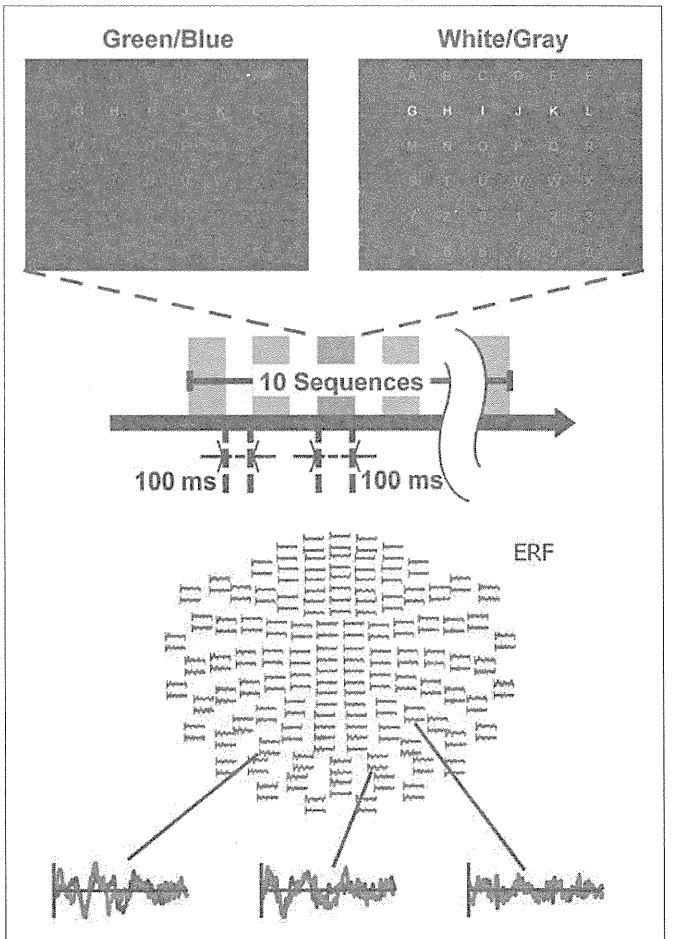

FIGURE 1 | Experimental setting. Two types of matrices were used: one for the green/blue (GB) condition and the other for the white/gray (WG) condition. Stimuli were presented in chromatic (GB) and luminance (WG) flickering patterns. Subjects were required to gaze at and attend to the target letter. Event-related fields from a representative subject under the GB condition are shown. The red lines indicate the averaged ERF elicited by the non-target stimuli, whereas the blue lines show the averaged ERF elicited by the target stimuli.

One complete cycle of six rows and six columns constituted a sequence (two target stimuli and 10 non-target stimuli), and 10 sequences constituted a trial. During a trial, participants were asked to focus on one of the icons as the target in the matrix. The target stimuli were presented as rare stimuli (20 target stimuli and 100 non-target stimuli in one trial) to elicit P300 responses (i.e., the oddball paradigm). We conducted six trials during a session under both the GB and WG conditions and simultaneously recorded MEG signals during each session. The order of the experimental conditions (GB or WG) was counterbalanced among participants. We thus recorded 120 segmented data points of the target and 600 segmented data points of the non-target from each participant in each condition.

MEG DATA ACQUISITION

For 306-channel whole-head MEG recording, we used a Neuromag Vectorview (Elekta AB, Helsinki, Finland). This system has 102 sensor triplets, with each triplet containing one magnetometer and two gradiometers. Brain activities were sensed and digitized at a rate of 1000 Hz and filtered with a band-pass filter of 0.1–330 Hz. Additionally, four head position indicator (HPI) coils were placed on the subjects' scalp to record head position relative to the MEG helmet at the beginning of each session. Three cardinal points (nasion, left and right preauricular) were digitized and used for co-registration with structural MRI data and spatial filtering.

MEG DATA ANALYSES

Sensor-based analyses

We preprocessed the wave data from 204 gradiometers, extracted using FieldTrip (Donders Centre for Cognitive Neuroimaging). These data were then filtered with Signal Space Projections (SSP) and 50-Hz notch and 100-Hz low-pass filters. As described in our previous studies (8, 10), filtered data from 800 ms of the MEG were segmented, starting at 100 ms before intensification. Data from the initial 100 ms (just before the intensification) were used for baseline correction.

We then computed the coherence using FieldTrip software (26). The coherence between left and right parieto-occipital channels was computed from the segmented data using only 204 gradiometers. The alpha band (8–12 Hz) was used as the target frequency. We computed the power spectrum density and cross-spectrum density. We combined the 204 gradiometers into 102 channels by calculating the norm. Using these spectra, we computed coherence between channels limited to the bilateral parieto-occipital area. Thus, the number of the channel combinations was 196 (14 × 14 channels). Then, we tested the differences in the coherence between the GB and WG conditions using a paired-sample t-test with a Bonferroni correction (**Figure 2**).

Voxel-based analyses

We preprocessed the wave data from the 204 gradiometers and 102 magnetometers using FieldTrip software. These data were filtered with SSP and 50-Hz notch and 100-Hz low-pass filters. As

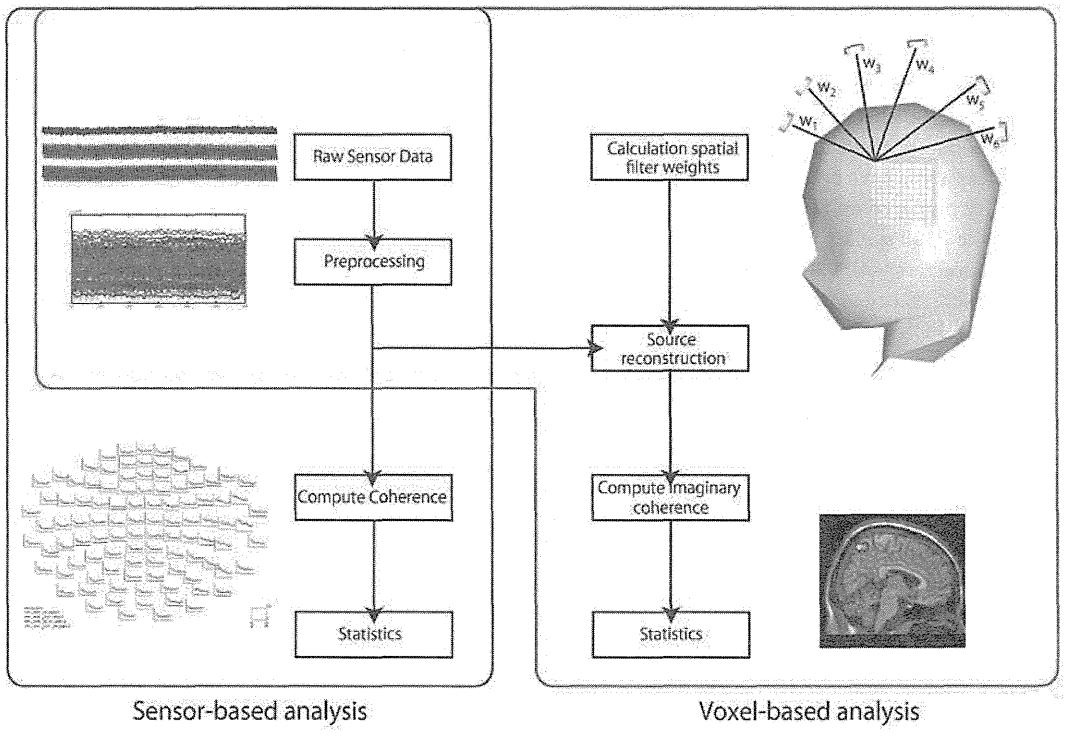

FIGURE 2 | Data processing. Two processes were used: sensor-based analysis and voxel-based analysis. In the sensor-based analysis, the coherence between sensors was computed. In the voxel-based analysis, the sensor data were first projected to voxel space. Second, the mean imaginary coherence was computed. Finally, the projected data were transformed to a standard brain.

described in our previous studies (8, 10), filtered data from 800 ms of the MEG were segmented, starting at 100 ms before intensification. Data from the initial 100 ms were used for baseline correction. We specifically focused on around 10 Hz for analysis as explained in the Section "Introduction."

To project the sensor data to voxel space, we used an adaptive beamformer (27) to transform to individual voxel space. The T1 MRI of each participant was used for co-registration. The voxel size was 7.7 mm × 7.7 mm × 7.7 mm. To clarify functional connectivities, we applied imaginary coherence (20–22). Imaginary coherence allows unambiguous detection of brain interaction from EEG/MEG data by retaining only the imaginary part of the cross-spectrum. In the voxel-based analysis, we evaluated the MIC as an index of functional connectivity. MIC is the average coherence between a seed voxel and all the other voxels across the entire brain (≥ 0). With MIC, we estimated the magnitude of connectivities between the seed voxel and all the other voxels. Voxel data were normalized using SPM8 in MATLAB (MathWorks, Natick, MA, USA). We used the canonical MRI data to create a transformation matrix. We computed MIC from the segmented data of target and non-target for all voxels under each condition. We mapped the difference between MIC of the target and non-target at all voxels (MIC map). We evaluate the differences in the MIC map between the GB and WG conditions. In our previous EEG–fMRI study, we showed greater activation in the parieto-occipital areas under chromatic conditions, and we observed the peak fMRI activation at ($x = 32, y = -53, z = 41$) (11). We thus defined a 10-mm-radius spherical ROI following the study. Differences between the two MIC maps (GB versus WG) obtained from each individual ($n = 12$) were tested using a paired-sample t-test (**Figure 2**).

RE-ANALYSES OF P300-BCI EEG DATA

We re-analyzed previous P300-BCI EEG data ($n = 20$) to evaluate relationships between coherence and accuracy with the P300-BCI. The data used in this reanalysis have been published previously (8, 10). In these studies, we prepared an 8 × 10 hiragana (a Japanese character) matrix for the P300 speller, and subjects were required to input 15 hiragana characters with P300-BCI under GB and WG conditions. These data were recorded from eight electrodes (Fz, Cz, P3, Pz, P4, PO7, Oz, and PO8). The data were segmented in the same manner as in the MEG experiments, and the same target frequency was used. The segmented data were also used for P300-BCI evaluation. We used the waveform as a feature vector. The segmented data using a sampling rate of 21 Hz correspond to 15 data points, and data were collected with eight EEG channels. Thus, the feature vector had 120 dimensions. We used Fischer's linear discriminant analysis for the feature vector to obtain classification accuracy. We evaluated the correlation between the coherence of the EEG signals and accuracy of the P300-BCI.

RESULTS

MEG DATA ANALYSES

Sensor-based analyses

We analyzed the alpha-band coherence between MEG sensors of the bilateral parieto-occipital areas (**Figure 3**). We set the ROI in the parieto-occipital area because P300 responses had been preferentially observed in these areas according to previous reports using EEG and fMRI data (11, 28–31). Further, there are reports showing alpha-band parieto-occipital activation and coherence in response to meaningful visual stimuli (19).

The alpha-band coherence between a sensor combination [ch2622 + 2623 and ch1732 + 1733, two-tailed $t(11) = 8.07$, $p = 0.0006$, Bonferroni-corrected] was significantly greater under the GB condition than under the WG condition. In contrast, significantly greater coherence was not observed under the WG condition compared to the GB condition.

Voxel-based analyses

Figure 4 shows the difference in the MIC of the power between the GB and WG conditions. Significantly greater coherence was observed in the right inferior parietal lobule under the GB [$x = 42$, $y = -48$, $z = 44$; two-tailed $t(11) = 3.60$, $p = 0.0253$ Bonferroni-corrected] than under the WG condition. The power distribution in this voxel did not show significant difference [two-tailed $t(11) = 0.05$, $p = 0.9595$, uncorrected]. In the WG condition, no coherence greater than that of the GB condition was observed [two-tailed $t(11) = 0.01$, $p = 1.0$, uncorrected].

RE-ANALYSES OF P300-BCI EEG DATA

We re-analyzed the P300-BCI EEG data (8, 10) and computed the coherence between left (P3, PO7) and right channels (P4, PO8); this was done because, in our previous studies, we observed that the electrodes in the parieto-occipital areas play an important role in the P300-BCI operation. We performed a coherence analysis with the EEG data too because a close relationship between MEG data coherence and EEG data coherence has been reported (32). The change in coherence from the non-target to the target condition was used for analysis. A significant correlation was observed between the mean accuracy of each subject and the difference in coherence (target–non-target) (between P4 and PO7; Pearson's coefficient of correlation, $p = 0.009$, uncorrected) under the GB condition (**Figure 5**). No significant correlation was observed

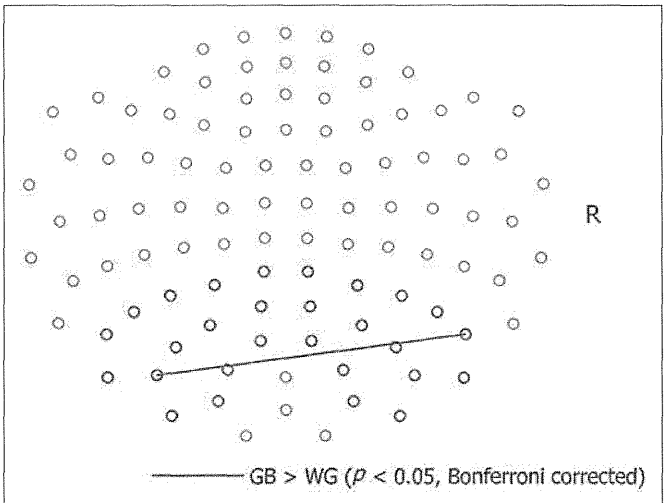

FIGURE 3 | Sensor-based coherence. The blue lines indicate significantly greater coherence between sensors under the GB than under the WG condition. Significantly greater coherence ($p < 0.05$, with Bonferroni correction) under the WG than under the GB condition was not observed.

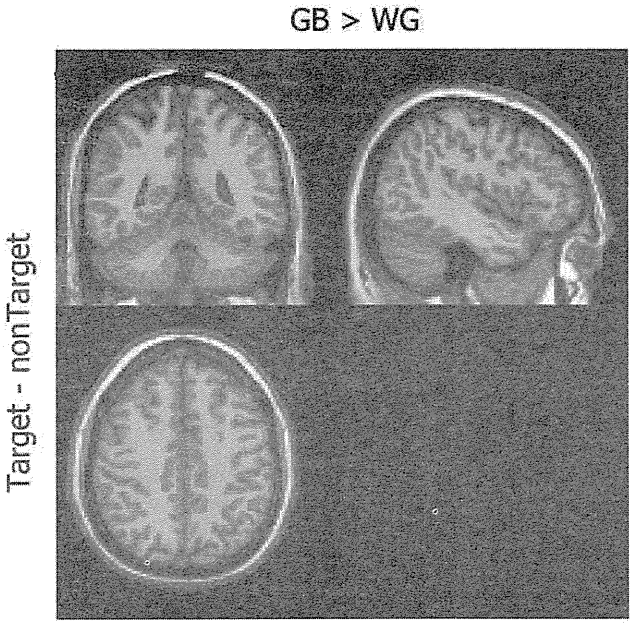

FIGURE 4 | Mean imaginary coherence. The inferior parietal area showed higher MIC under the GB than under the WG condition (GB > WG).

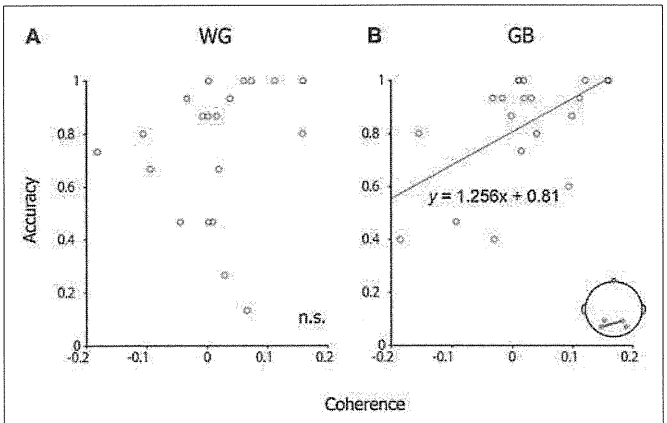

FIGURE 5 | Scatter plot of coherence and accuracy. **(A)** Scatter plot of coherence and accuracy under the WG condition. **(B)** Scatter plot of coherence and accuracy under the GB condition. The horizontal axis shows coherence between P4 and Po7, and the vertical axis shows accuracy during the P300-BCI task. A significant correlation was observed under the GB condition.

between other channel combinations (P3 and P4, P3 and PO8, PO7 and PO8). No significant correlation was observed during WG conditions.

We further investigated the relationship between coherence and correct/incorrect responses at the single-trial level. We calculated the coherence between P4 and PO7 in each trial, and then the data were evaluated separately with respect to correct or incorrect responses. This analysis revealed a significant difference between the correct and incorrect responses in the GB condition [two-tailed $t(298) = 3.80, p < 0.001$], but not in the WG condition [two-tailed $t(298) = 1.79, p = 0.0746$].

DISCUSSION

Magnetoencephalography activity during P300-BCI use was investigated. When comparing functional connectivity between the right and left occipital channels, significantly greater functional connectivity in the alpha band was observed under the GB than under the WG flicker matrix condition. Application of MIC revealed that coherence was significantly greater in the right posterior parietal cortex under the GB than under the WG condition. Re-analysis of previous EEG-based P300-BCI data showed a significant correlation between the power of the coherence between bilateral parieto-occipital electrodes and performance accuracy.

COHERENT ACTIVITY AND GB FLICKER

In the sensor-based analysis, by specifically focusing on the alpha band, according to former reports (13, 14, 19), greater coherence between bilateral parieto-occipital areas was observed under the GB than under the WG condition. This result suggests that chromatic stimuli elicited activity in the parietal attentional system more effectively than conventional WG stimuli did. These results are also consistent with our previous study, in which we showed that EEG channels in the lateral parietal areas were more important for P300-BCI operation (33).

We also investigated differences between the GB and WG conditions in the MIC of the power. Significantly greater coherence was observed in the right parieto-occipital area under the GB than under the WG condition (11). In a previous fMRI study, chromatic visual stimuli activated the right occipital and parietal areas (34). In our earlier study, we made simultaneous EEG–fMRI recordings during GB and WG conditions, and the peak of the positive wave in the EEG data was detected under both conditions. The peak amplitudes were larger at the parietal and occipital electrodes, particularly in the late components, under the GB versus the WG condition. fMRI data showed activation in the bilateral parietal and occipital cortices, and these areas, particularly in the right hemisphere, were more activated under the GB than under the WG condition (11). As discussed in that paper, the right hemisphere may be more involved in color detection. Indeed, a psychophysical study suggested the superiority of the right hemisphere for detecting color (35).

P300-BCI ACCURACY AND COHERENT ACTIVITY

Increasing accuracy in P300-BCI operation is a major topic in this field of research. The classification methods of EEG and the optimization of the target of classification have been investigated extensively, and analyses relying on stepwise LDA (36), ICA (37) and common spatial patterns have been applied. Other studies have tested various aspects of visual stimuli, such as their position, pattern, and number to increase accuracy (38–41).

Our re-analysis of previous EEG-based P300-BCI data showed a significant correlation between the power of the coherence between the bilateral parieto-occipital cortices and performance accuracy, suggesting that increasing the power of the coherence between bilateral parieto-occipital cortices may be key to increasing the accuracy of the P300-BCI operation. GB flicker may contribute to increasing the power of the coherence. In this study,

we investigated the effects of chromatic stimuli for the P300-BCI, and we found coherence in the right inferior parietal lobule. These coherence features may be useful for classification to improve the accuracy of the P300-BCI, and the coherence values may be usable for neurofeedback training with the P300-BCI.

There are several limitations to this study. First, we were not able to evaluate P300-BCI accuracy during the MEG experiments because, as reported in a previous MEG–BMI study (42), the sensor location showing the highest P300-BCI accuracy varies among participants. Because of this variation, it is difficult to differentiate between the effect of channel selection and the effect of chromatic stimuli when examining the relationship between the imaginary coherence of the MEG data and the P300 performance. Second, we did not collect simultaneous EEG data, and did not evaluate online and offline performance during the P300 tasks. These activities were omitted because a real-time EEG system was not available, and also because the positions of the EEG electrodes available in the simultaneous EEG–MEG recording system are different than in the conventional P300-BCI system. However, it is important to note that a positive relationship was observed between P300 performance and coherence of the EEG data, which was revealed in the comparison between the GB flickering condition and the WG flickering condition.

In our previous research, we found that chromatic visual stimuli improved accuracy in P300-BCI operations (8); in this previous study, the EEG waveform was used to classify the target stimuli. Furthermore, in our previous EEG–fMRI study, we found that peak EEG amplitudes were larger under the GB condition than under the WG condition at the parietal and occipital electrodes (11). These results suggest the ease with which changes can be detected under the GB flicker condition, which is consistent with Polich's observation that the P300 amplitude is smaller in response to more difficult than to easier tasks (43). Thus, the GB visual stimuli may have allowed participants to detect changes more readily. Furthermore, inter-hemispheric neuronal coherence was improved when the object was recognized (19). We suggest that our chromatic stimuli preferentially elicited right-dominant activation in cooperation with the coherent activities of the bilateral occipital and parietal areas. Taken together, these data support the conclusion that coherent activity in the bilateral parieto-occipital cortices may play a significant role in effectively driving P300-BCI.

ACKNOWLEDGMENTS

This study was supported, in part, by a MHLW grant (BMI), a MEXT/SRPBS grant, and a MEXT grant (#23300151). We thank Dr. S. Ikegami and M. Wada for their help and Dr. Y. Nakajima for his continuous encouragement.

REFERENCES

1. Birbaumer N, Ghanayim N, Hinterberger T, Iversen I, Kotchoubey B, Kubler A, et al. A spelling device for the paralysed. *Nature* (1999) **398**:297–8. doi:10.1038/18581
2. Wolpaw JR, McFarland DJ. Control of a two-dimensional movement signal by a noninvasive brain–computer interface in humans. *Proc Natl Acad Sci USA* (2004) **101**:17849–54. doi:10.1073/pnas.0403504101
3. Birbaumer N, Cohen LG. Brain–computer interfaces: communication and restoration of movement in paralysis. *J Physiol* (2007) **579**:621–36. doi:10.1113/jphysiol.2006.125633
4. Kansaku K. Brain-machine interfaces for persons with disabilities. In: Kansaku K, Cohen LG editors. *Systems Neuroscience and Rehabilitation.* Tokyo: Springer (2011). p. 19–33.
5. Farwell LA, Donchin E. Talking off the top of your head: toward a mental prosthesis utilizing event-related brain potentials. *Electroencephalogr Clin Neurophysiol* (1988) **70**:510–23. doi:10.1016/0013-4694(88)90149-6
6. Parra J, Lopes Da Silva FH, Stroink H, Kalitzin S. Is colour modulation an independent factor in human visual photosensitivity? *Brain* (2007) **130**:1679–89. doi:10.1093/brain/awm103
7. Takano K, Ikegami S, Komatsu T, Kansaku K. Green/blue flicker matrices for the P300 BCI improve the subjective feeling of comfort. *Neurosci Res* (2009) **65**(Suppl 1):S182. doi:10.1016/j.neures.2009.09.971
8. Takano K, Komatsu T, Hata N, Nakajima Y, Kansaku K. Visual stimuli for the P300 brain–computer interface: a comparison of white/gray and green/blue flicker matrices. *Clin Neurophysiol* (2009) **120**:1562–6. doi:10.1016/j.clinph.2009.06.002
9. Komatsu T, Hata N, Nakajima Y, Kansaku K. A non-training EEG-based BMI system for environmental control. *Neurosci Res Suppl* (2008) **1**(61):S251. doi:10.1016/j.neures.2008.05.002
10. Ikegami S, Takano K, Saeki N, Kansaku K. Operation of a P300-based brain–computer interface by individuals with cervical spinal cord injury. *Clin Neurophysiol* (2011) **122**:991–6. doi:10.1016/j.clinph.2010.08.021
11. Ikegami S, Takano K, Wada M, Saeki N, Kansaku K. Effect of the green/blue flicker matrix for P300-based brain–computer interface: an EEG-fMRI study. *Front Neurol* (2012) **3**:113. doi:10.3389/fneur.2012.00113
12. Siegel M, Donner TH, Engel AK. Spectral fingerprints of large-scale neuronal interactions. *Nat Rev Neurosci* (2012) **13**(2):121–34. doi:10.1038/nrn3137
13. Fu KM, Foxe JJ, Murray MM, Higgins BA, Javitt DC, Schroeder CE. Attention-dependent suppression of distracter visual input can be cross-modally cued as indexed by anticipatory parieto-occipital alpha-band oscillations. *Brain Res Cogn Brain Res* (2001) **12**:145–52. doi:10.1016/S0926-6410(01)00034-9
14. Mathewson KE, Gratton G, Fabiani M, Beck DM, Ro T. To see or not to see: prestimulus alpha phase predicts visual awareness. *J Neurosci* (2009) **29**:2725–32. doi:10.1523/JNEUROSCI.3963-08.2009
15. van Dijk H, Schoffelen JM, Oostenveld R, Jensen O. Prestimulus oscillatory activity in the alpha band predicts visual discrimination ability. *J Neurosci* (2008) **28**:1816–23. doi:10.1523/JNEUROSCI.1853-07.2008
16. Tonin L, Leeb R, Millan JR. Time-dependent approach for single trial classification of covert visuospatial attention. *J Neural Eng* (2012) **9**:045011. doi:10.1088/1741-2560/9/4/045011
17. Tonin L, Leeb A, Sobolewski A, Millan JR. An online EEG BCI based on covert visuospatial attention in absence of exogenous stimulation. *J Neural Eng* (2013) **10**:056007. doi:10.1088/1741-2560/10/5/056007
18. Treder MS, Bahramisharif A, Schmidt NM, Gerven MAJ, Blankertz B. Brain–computer interfacing using modulations of alpha activity induced by covert shifts of attention. *J Neuroeng Rehabil.* (2011) **8**:24. doi:10.1186/1743-0003-8-24
19. Mima T, Oluwatimilehin T, Hiraoka T, Hallett M. Transient interhemispheric neuronal synchrony correlates with object recognition. *J Neurosci* (2001) **21**:3942–8.
20. Nolte G, Bai O, Wheaton L, Mari Z, Vorbach S, Hallett M. Identifying true brain interaction from EEG data using the imaginary part of coherency. *Clin Neurophysiol* (2004) **115**:2292–307. doi:10.1016/j.clinph.2004.04.029
21. Nolte G, Holroyd T, Carver F, Coppola R, Hallett M. Localizing brain interactions from rhythmic EEG/MEG data. *Conf Proc IEEE Eng Med Biol Soc* (2004) **2**:998–1001. doi:10.1109/IEMBS.2004.1403330
22. Sekihara K, Owen JP, Trisno S, Nagarajan SS. Removal of spurious coherence in MEG source-space coherence analysis. *IEEE Trans Biomed Eng* (2011) **58**:3121–9. doi:10.1109/TBME.2011.2162514
23. Martino J, Honma SM, Findlay AM, Guggisberg AG, Owen JP, Kirsch HE, et al. Resting functional connectivity in patients with brain tumors in eloquent areas. *Ann Neurol* (2011) **69**(3):521–32. doi:10.1002/ana.22167
24. Tarapore PE, Martino J, Guggisberg AG, Owen J, Honma SM, Findlay A, et al. Magnetoencephalographic imaging of resting-state functional connectivity predicts postsurgical neurological outcome in brain gliomas. *Neurosurgery* (2012) **71**(5):1012. doi:10.1227/NEU.0b013e31826d2b78
25. Guggisberg AG, Honma SM, Findlay AM, Dalal SS, Kirsch HE, Berger MS, et al. Mapping functional connectivity in patients with brain lesions. *Ann Neurol* (2008) **63**:193–203. doi:10.1002/ana.21224

26. Oostenveld R, Fries P, Maris E, Schoffelen JM. FieldTrip: open source software for advanced analysis of MEG, EEG, and invasive electrophysiological data. *Comput Intell Neurosci* (2011) **2011**:156869. doi:10.1155/2011/156869
27. Sekihara K, Nagarajan SS. *Adaptive Spatial Filters for Electromagnetic Brain Imaging*. Berlin: Springer Verlag (2008).
28. Kiss I, Dashieff RM, Lordeon P. A parieto-occipital generator for P300: evidence from human intracranial recordings. *Int J Neurosci* (1989) **49**:133–9. doi:10.3109/00207458909087048
29. Clark VP, Fannon S, Lai S, Benson R, Bauer L. Responses to rare visual target and distractor stimuli using event-related fMRI. *J Neurophysiol* (2000) **83**:3133–9.
30. Bledowski C, Prvulovic D, Hoechstetter K, Scherg M, Wibral M, Goebel R, et al. Localizing P300 generators in visual target and distractor processing: a combined event-related potential and functional magnetic resonance imaging study. *J Neurosci* (2004) **24**:9353–60. doi:10.1523/JNEUROSCI.1897-04.2004
31. Babiloni C, Vecchio F, Miriello M, Romani GL, Rossini PM. Visuo-spatial consciousness and parieto-occipital areas: a high-resolution EEG study. *Cereb Cortex* (2006) **16**:37–46. doi:10.1093/cercor/bhi082
32. Schack B, Grieszbach G, Nowak H, Krause W. The sensitivity of instantaneous coherence for considering elementary comparison processing. Part II: similarities and differences between EEG and MEG coherences. *Int J Psychophysiol* (1999) **31**:241–59. doi:10.1016/S0167-8760(98)00053-1
33. Takano K, Hata N, Kansaku K. Towards intelligent environments: an augmented reality-brain-machine interface operated with a see-through head-mount display. *Front Neurosci* (2011) **5**:60. doi:10.3389/fnins.2011.00060
34. Bramao I, Faisca L, Forkstam C, Reis A, Petersson KM. Cortical brain regions associated with color processing: an FMRI study. *Open Neuroimag J* (2011) **4**:164–73. doi:10.2174/1874440001004010164
35. Sasaki H, Morimoto A, Nishio A, Matsuura S. Right hemisphere specialization for color detection. *Brain Cogn* (2007) **64**:282–9. doi:10.1016/j.bandc.2007.03.010
36. Krusienski DJ, Sellers EW, Mcfarland DJ, Vaughan TM, Wolpaw JR. Toward enhanced P300 speller performance. *J Neurosci Methods* (2008) **167**:15–21. doi:10.1016/j.jneumeth.2007.07.017
37. Xu N, Gao X, Hong B, Miao X, Gao S, Yang F. BCI competition 2003 – data set IIb: enhancing P300 wave detection using ICA-based subspace projections for BCI applications. *IEEE Trans Biomed Eng* (2004) **51**:1067–72. doi:10.1109/TBME.2004.826699
38. Townsend G, Lapallo BK, Boulay CB, Krusienski DJ, Frye GE, Hauser CK, et al. A novel P300-based brain–computer interface stimulus presentation paradigm: moving beyond rows and columns. *Clin Neurophysiol* (2010) **121**:1109–20. doi:10.1016/j.clinph.2010.01.030
39. Treder MS, Blankertz B. (C)overt attention and visual speller design in an ERP-based brain–computer interface. *Behav Brain Funct* (2010) **6**:28. doi:10.1186/1744-9081-6-28
40. Jin J, Allison BZ, Sellers EW, Brunner C, Horki P, Wang X, et al. An adaptive P300-based control system. *J Neural Eng* (2011) **8**:036006. doi:10.1088/1741-2560/8/3/036006
41. Aloise F, Arico P, Schettini F, Riccio A, Salinari S, Mattia D, et al. A covert attention P300-based brain–computer interface: Geospell. *Ergonomics* (2012) **55**:538–51. doi:10.1080/00140139.2012.661084
42. Bianchi L, Sami S, Hillebrand A, Fawcett IP, Quitadamo LR, Seri S. Which physiological components are more suitable for visual ERP based brain–computer interface? A preliminary MEG/EEG study. *Brain Topogr* (2010) **23**:180–5. doi:10.1007/s10548-010-0143-0
43. Polich J. Task difficulty, probability, and inter-stimulus interval as determinants of P300 from auditory stimuli. *Electroencephalogr Clin Neurophysiol* (1987) **68**:311–20. doi:10.1016/0168-5597(87)90052-9

Conflict of Interest Statement: The authors declare that the research was conducted in the absence of any commercial or financial relationships that could be construed as a potential conflict of interest.

Received: 20 September 2013; paper pending published: 06 November 2013; accepted: 01 May 2014; published online: 15 May 2014.

Citation: Takano K, Ora H, Sekihara K, Iwaki S and Kansaku K (2014) Coherent activity in bilateral parieto-occipital cortices during P300-BCI operation. Front. Neurol. 5:74. doi: 10.3389/fneur.2014.00074

This article was submitted to Neuroprosthetics, a section of the journal Frontiers in Neurology.

平成 26 年度厚生労働科学研究費補助金（障害者対策総合研究事業（身体・知的等分野））
「ブレインーマシン・インターフェイス（BMI）による障害者自立支援機器の開発」

総括・分担研究報告書

発行者　　中島　八十一（研究代表者：国立障害者リハビリテーションセンター）
〒359-8555　埼玉県所沢市並木 4-1